Preparation and characterization of a low transition temperature mixture choline chloride-acetylsalicylic acid for dispersive liquid-liquid microextraction-based applications.

Pierpaolo Tomai[a], Paola D'Angelo[a], Ingmar Persson[b], Andrea Martinelli[a], Valerio Di Lisio[a], Roberta Curini[a], Chiara Fanali[c], Alessandra Gentili[a]*

[a] *Department of Chemistry "Sapienza" University" of Rome, P.le Aldo Moro 5, 00185, Rome, Italy.*

[b] *Department of Chemistry, Swedish University of Agricultural Sciences, P.O. Box 7015, 75007 Uppsala, Sweden*

[c]*Unit of Food Science and Nutrition, Department of Medicine, Università Campus Bio-Medico di Roma, Via Alvaro del Portillo 21, 00128, Rome, Italy.*

*Corresponding author: Fax number: + 39-06-490631.

E-mail address: alessandra.gentili@uniroma1.it

Abstract

This paper illustrates the preparation of a low transition temperature mixture (LTTM), resulting from the heat-mixing of choline chloride and acetylsalicylic acid in a molar ratio 1:2 ($ChCl(ASA)_2$). The mixture appears as a clear viscous liquid at room-temperature, denser than water (1.20 ± 0.01 g mL^{-1}). Differential scanning calorimetry (DSC) provided crucial evidence to classify the mixture as a LTTM rather than as a deep eutectic solvent (DES) since it revealed an intense glass transition at -37 °C. Such a result is in agreement with the lack of any long-distance order, observed by means of large-angle X-ray scattering (LAXS). As further confirmation, the infrared spectra of the LTTM and the parent moieties showed a marked difference arising from the amorphous nature of $ChCl(ASA)_2$ and from a redistribution of H-bonds among the functional groups of the molecules. Electrospray-mass spectrometry (ESI-MS) also allowed the identification of some characteristic ion species. Due to its immiscibility with water, $ChCl(ASA)_2$ was tested as an extraction solvent for dispersive liquid-liquid microextraction (DLLME), in alternative to the conventional chlorinated solvents. To this end, 24 pesticides were used as model compounds and extracted from surface water samples (5 mL) with recoveries ranging from 22 to 92 % and relative standard deviations lower than 15 %. All extracts were analyzed using high-performance liquid chromatography-tandem mass spectrometry (HPLC-MS/MS). Key parameters affecting the recovery rates were carefully optimized: volume of extracting solvent, type and volume of dispersing solvent, the volume of the aqueous sample, LTTM dispersion procedure, extraction time. After optimization and validation, the method was applied to analyze water samples from the River Tiber, finding dodine and dimetomorph at low μg L^{-1} concentration levels.

Keywords: low transition temperature mixture; deep eutectic solvents; dispersive liquid-liquid microextraction; sample preparation; environmental samples; LC-MS.

Deep eutectic solvents (DESs)[1] and low transition temperature mixtures (LTTMs)[2] are neoteric solvents[3] which have recently aroused the keen interest of the scientific community for displaying the same physical properties of ionic liquids (ILs), with which they are closely related. Their singular capacity of solubilizing some inorganic and organic compounds, refractory to the conventional molecular solvents, has made their use especially captivating for applications in electrochemistry, catalysis and separation processes.[2,4]

The term DES was conceived by Abbot and his co-workers in 2003[5] to describe any mixture with a marked ("deep") drop of the melting point in comparison with the values of the individual solid components. Actually, some of such mixtures were already known in the 50s of the twentieth century.[6-8] Nowadays, DESs are systematically described by the general formula $Cat^+X^-\square zY$,[2] where Cat^+X^- is a salt, often composed by a quaternary ammonium cation and a Lewis base as counterion (e.g. Cl^-); Y is a Lewis or Brønsted acid which acts as complexing agent and z is the number of Y molecules. Depending on the nature of Y, DESs have been classified in four main classes:[2] in all cases, Y tends to complex with X^- to give $Cat^+[XY]^-$; however, the complexation of Y with Cat^+ to give $[CatY]^+X^-$ is also possible.[9] Among such classes, the real novelty is represented by the so-called type-III DESs[2] because they are the result of a self-association mediated by H-bonds mainly between X^- and Y, where X^- and Y act as an acceptor (HBA) and a donor (HBD) of H-bond, respectively. So far, the most frequently studied DESs have been those resulting from the mixing of ChCl with an amide or alcohol (e.g. urea or glycerol) in exact molar ratios, usually 1:1, 1:2 or 1:3. For such mixtures, the decrease in the melting point has been ascribed to the strength of the anionic H-bond (e.g. $Cl^-\cdots HBD$),[2,10] responsible for charge delocalization occurring on Cl^- and consequent weakening of the Ch^+Cl^- electrostatic interaction. In general, it has been observed that the stronger the H-bond, the deeper the depression of freezing point. In particular, it has been hypothesized that a crucial role would be played by the pKa values of HBD and HBA.[3,11] In fact, since H-bond results from both electrostatic and covalent contributions, its strength increases with

the covalent component, namely as the difference of donor-acceptor acidic constants approaches zero ($\Delta pK_a \sim 0$).[11,12]

At the present moment, the research into DESs is still in its infancy and several studies are in progress to unravel mechanisms of both eutectic formation and action as solvent systems. For the same reasons, much work is still to be done to adequately characterize DESs and LTTMs and avoid using the two terms indiscriminately.[13] LTTMs are similar to DESs, but instead of having a melting/freezing point, they display a glass transition.[3] Like DESs, LTTMs are obtainable with a high degree of purity, simply mixing the two solid components under moderate heating. Method of preparation, cost-effectiveness of starting products (ChCl and many HBDs are available around 2-4 € Kg^{-1}) and real recyclability (the mixture can be disrupted by dilution leading to the recrystallization of both or one of the initial compounds) make these solvents appropriate to meet the circular economy requirements.

The use of neoteric solvents is an attractive alternative to the classical molecular solvents or the unique solution to dissolve poorly soluble solutes. So far, $ChCl(urea)_2$ and $ChCl(phenol)_3$[14] have been the main DESs used for such purposes. Nevertheless, considering the very high number of theoretical combinations (around 10^6), a variety of DESs and LTTMs can be designed with physicochemical properties advantageously tailored. And what is more, such properties, including polarity, viscosity and aptitude to dissolve materials of special interest, can further be modulated by varying the ratio between the selected HBA and HBD. Compared to ILs, the stoichiometry flexibility is an additional advantage.

The applications of neoteric solvents within the framework of sample preparation have still been limited. However, it is necessary to underline how, in just less than three years, there have been published about fifty papers dealing with the use of DESs for the liquid-liquid extraction (LLE) of biomolecules or contaminants from matrices of aqueous or oily nature.[14] Most of these applications involve liquid-phase microextraction (LPM) techniques.[14-24] Among them, dispersive liquid-liquid microextraction (DLLME) stands out for its simplicity, inexpensiveness, rapidity, high enrichment

factor (up to 100), and great extraction efficiency. Assadi et al. came up with it in 2006[25] with the major aim of significantly reducing the organic solvent consumption. DLLME is based on the use of a ternary solvent system, consisting of: *i*) an aqueous sample containing the analytes (a few milliliters), *ii*) an extraction phase immiscible with water (usually a few microliters of a chlorinated solvent) and *iii*) a dispersing phase (usually from few hundred to one thousand microliters of methanol, acetone, etc.). Basically, the rapid injection of the two organic solvents into the aqueous sample generates a cloudy solution in which the extractant is finely dispersed in the form of micro-drops. Since the interfacial surface area is very high, the analyte mass transfer occurs rapidly. The subsequent centrifugation leads to the sedimentation of the chlorinated solvent, which is then recovered with a micro-syringe.

To the best of our knowledge, no work involving the explicit use of LTTMs as extraction systems for DLLME-based applications has been published so far. The aim of this work is to describe the advantages in using the hydrophobic LTTM prepared and characterized for the first time in our lab. This LTTM, which appears as a transparent viscous liquid at room temperature, is obtained by heat-mixing ChCl and acetylsalicylic acid (ASA) in a molar ratio 1:2. The two starting solid materials are low price available, biocompatible and potentially recoverable by breaking the LTTM H-bond networks. The mixture composition was designed to avoid typical drawbacks of chlorinated solvents such as toxicity, solvent volatility, and poor compatibility with the mobile phase composition used for reversed-phase liquid chromatography (RP-LC). Characterization by means of differential scanning calorimetry (DSC), infrared spectroscopy, ESI-MS and large-angle X-ray scattering (LAXS) allowed us to classify the mixture as an LTTM and to investigate its physicochemical properties, also in terms of solvent abilities. To this end, $ChCl(ASA)_2$ was experimented as an extractant for an environmental DLLME-based application. Its extraction efficiency was assessed by recovering 24 pesticides, belonging to several chemical classes and known to be common environmental pollutants, from surface water samples.

EXPERIMENTAL SECTION

Chemicals, Materials and Solutions.

Authentic standards of acetamiprid, azoxystrobine, boscalid, buprofezin, chlorpyrifos, chlorpyrifos-methyl, clofentezine, dimetomorph, dodine, fluquinconazole, fludioxonil, hexythiazox, imidacloprid, methyl-thiophanate, methoxyfenozide, myclobutanil, penconazole, propiconazole, pyraclostrobin, pyriproxyfen, pyridaben, spirotetramat, tebuconazole, and tebufenpyrad were acquired from Aldrich–Fluka–Sigma S.r.l. (Milan, Italy). All standards were more than 98% pure. **Table S-1** in the Supporting Information lists all 24 pesticides with the physicochemical characteristics of interest for this study.

Acetonitrile (AcCN), methanol (MeOH), ethanol (EtOH), chloroform ($CHCl_3$), dimethyl sulfoxide (DMSO), toluene and tetrahydrofuran (THF), ChCl, ASA, phenol (Ph) were obtained from Sigma-Aldrich S.r.l. Ultrapure water was produced from a Milli-Q water generator (Millipore, Bedford, MA, USA).

Individual stock solutions were prepared by dissolving weighed standard amounts in methanol (most analytes) or toluene (clofentezine, dimetomorph, fluquinconazole and pyraclostrobin) at a concentration of 1 mg mL^{-1}. Only solutions of propiconazole and dimetomorph were at 0.5 mg mL^{-1}, while that of fluquinconazole at 10 mg mL^{-1}. Working composite standard solutions were obtained by diluting a mix of the individual ones with methanol at concentrations depending on the purpose. All standards and solutions were kept at 4 °C in the darkness when unused.

Environmental Samples. Surface water samples were gathered in 5-L dark glass bottles from Lake Martignano and from four different sites along the River Tiber (**Figure S-1**): Oasi di Farfa (a natural area, 50 km north of Rome); Tor di Quinto (northern suburb of Rome); Tiber Island in the center of Rome; Marconi Bridge (southern suburb of Rome). Before the extraction, all samples were filtered through 1.2 μm Whatman glass microfiber filters (Whatman International Ltd, Maidstone, UK) and held at 4 °C. Preliminary analyses showed that samples from Lake Martignano could be used as blanks to perform the method validation.

Preparation of ChCl(ASA)$_2$ mixture. Preliminarily to the preparation of ChCl(ASA)$_2$, ChCl and ASA were dried in a muffle oven at 90 °C for 24 h. Once completed the drying process, 1.107 g of ChCl and 2.858 g of ASA were quickly weighed in a 25-mL weighing bottle and blended with a spatula. Then, the weighing bottle was closed and heated on a heating plate at a temperature of about 80 °C for 1 h. These conditions avoided triggering decomposition processes (see subsection *Thermogravimetric analysis*). The mixture (~ 3 mL) was then allowed to cool at room temperature, appearing as a transparent viscous liquid. Once cooled to room temperature, MeOH (578 µL) was added and mixed quickly with a spatula to reduce viscosity and favor its sampling with a micro-syringe (the molar ratio ChCl(ASA)$_2$:MeOH was 1:1.8). The overall mixture, referred to as ChCl(ASA)$_2$MeOH, had a total volume of 3.5 mL, suitable for at least 35 extractions.

Extraction procedure. The different steps of the extraction procedure are schematically shown in **Figure 1**. A centrifuge tube (15 mL falcon) was filled with 5 mL of surface water. 100 µL of ChCl(ASA)$_2$MeOH (extraction solvent) and 1 mL of THF (dispersing solvent) were taken with Hamilton syringes and sequentially injected into the aqueous sample. After stirring on a vortex mixer for 2 min, the aqueous solution appeared cloudy due to the fine dispersion achieved. The mixture was then centrifuged at 12500 g for 10 min at room temperature. After centrifugation, a phase separation was observed. The ChCl(ASA)$_2$ mixture, being denser, settled on the bottom of the tube and was taken with a micro-syringe (70 µL volume of final extract). After dilution with 30 µL of MeOH (100 µL of total final volume), 10 µL were injected for the HPLC-MS analysis.

High-performance liquid chromatography-tandem mass spectrometry. The HPLC apparatus was a Perkin Elmer series 200 binary pump equipped with an autosampler (Perkin Elmer, Norwalk, CT). The analytes were chromatographed on a XTerra C_{18} (5 µm) column (4.6 x 250 mm), protected by a guard column (Waters, Milford, Massachusetts, USA). Water (phase A) and AcN (phase B), both 5 mM in formic acid, were used as mobile phases. At a flow rate of 1 mL min^{-1}, a gradient elution was carried out increasing the percentage of B from 35% to 100% in 16 min and, then, keeping B at 100% for 4 min. A post-column T-valve split the mobile phase, leading 200 µL

min^{-1} into the ESI source of the mass spectrometer. After each injection, the autosampler needle was washed with AcN.

The triple quadrupole mass spectrometer was a PE-Sciex API-3000® (Perkin Elmer Sciex Toronto, Canada), equipped with an ESI source operated in positive ionization. The capillary voltage was +4500V. High purity nitrogen was used as curtain and collision gas, while air as nebulizer and drying gas. The last one was heated by setting the source heather temperature at 350°C. The full width at half maximum (FWHM) was set at *m/z* 0.7 ± 0.1 in each mass-resolving quadrupole to operate with a unit resolution. The scheduled multiple reaction monitoring (SMRM) mode was used for the analyte quantification, setting an MRM detection window of 120 s in the retention window characteristic of each analyte (t_r ± 60 s) and a target scan time of 2 s. Two SMRM transitions were selected per analyte, for a total of 48 ion currents monitored with a pause time of 5 ms. All the LC-MS parameters, useful for identification and quantification, are listed in **Table S-2**. The LC–MS data were processed by Analyst® 1.5 Software (AB Sciex).

Thermogravimetric analysis (TGA). The thermal stability of $ChCl(ASA)_2$, ChCl and ASA were investigated by thermogravimetric analysis (TGA) carried out by using a Mettler Toledo TG50 measuring module linked to a Mettler Toledo TC 10 interface. About 10 mg of dried sample (ChCl, ASA or $ChCl(ASA)_2$) were weighted in a ceramic pan which, after being closed with a lid, was rapidly placed in the measuring furnace, purged with 30 mL min^{-1} nitrogen flux. TGA curves were acquired during the heating from 30 °C to 500 °C at 10 °C min^{-1}.

Differential scanning calorimetry (DSC). The thermal properties of $ChCl(ASA)_2$ were characterized by DSC by using a Mettler Toledo DSC 822e instrument (Mettler Toledo, Greifensee, Switzerland). About 2 mg of sample was rapidly weighed in an aluminum pan and sealed to avoid water absorption. The sample was cooled from 20 to -150 °C and, then, heated up to 20 °C, using a scanning rate of 10 °C min^{-1}. The furnace was purged by dry nitrogen at a flow rate of 30 ml min^{-1}.

Infrared spectroscopy. FT-IR spectra of ChCl, ASA and neoteric solvent were acquired in attenuated total reflection mode (ATR) by using a Thermo Nicolet 6700 instrument (Thermo

Scientific, MA, USA), equipped with a Golden Gate diamond single reflection device (Specac LTD, England). The ATR-FTIR spectra were collected co-adding 100 scans in the range 4000–650 cm^{-1} at a resolution of 2 cm^{-1}.

Large-angle X-ray scattering (LAXS). A large-angle θ–θ diffractometer was employed to measure the scattering of MoKa radiation (λ=0.7107) on the free surfaces of a liquid mixture of $ChCl(ASA)_2$ (ρ=1.20 $g \cdot cm^{-3}$, and μ=2.022 cm^{-1}) and liquid mixture of $ChCl(ASA)_2$ diluted with MeOH ($ChCl(ASA)_2$ - MeOH 1:1.8 molar ratio) (ρ=1.23 $g \cdot cm^{-3}$, and μ=1.919 cm^{-1}). The solutions were contained in a Teflon cuvette with an air-tight radiation shielding with beryllium windows. The scattered radiation was monochromatized in a focusing LiF crystal monochromator and the intensity was measured at 450 discrete points in the range $1<\theta<65^o$ (the scattering angle is 2θ). 100000 counts were accumulated at each preset angle, and the whole angular range was scanned twice, which corresponds to a statistical error of about 0.3%. The divergence of the primary X-ray beam was limited by 1 or ¼° slits for different θ regions with some parts of the data overlapping for scaling purposes. All of the data treatment was performed with the KURVLR program.[26] All the details in the data treatment approach can be found elsewhere.[27] The experimental intensities were normalized to a stoichiometric unit of volume containing one chlorine atom, using the scattering factors f for neutral atoms, including corrections for anomalous dispersion $\Delta f'$ and $\Delta f''$,[28] and values for Compton scattering.[29,30] Least-squares refinements of the model parameters were carried out by means of the STEPLR program,[31] where the expression $U = \Sigma[s \cdot i_{exp}(s) - s \cdot i_{calc}(s)]^2$ is minimized. In order to obtain a better alignment of the intensity function before the refinements, a Fourier back-transformation procedure was used to correct the $i_{exp}(s)$ functions by removing spurious non-physical peaks below 1.2 Å in the experimental radial distribution function (RDF).[32] Corrections due to the low absorptions coefficients, μ, have been applied.[26]

RESULTS AND DISCUSSION

Preparation of some neoteric solvents. A series of mixtures (see **Table 1** and **Figure 2**) were prepared to be evaluated as extractants in a DLLME-based application. The mixture $ChCl(Ph)_3$, already known in the literature,[14] turned into liquid directly at room temperature by stirring the starting solid components with a spatula for 3-5 minutes. Both mixtures of ChCl and salicylic acid (SA) solidified when cooled to room temperature; they probably give rise neither to DES nor to LTTM because SA prefers forming an intramolecular H-bond (six-term ring) rather than acting as a HBD with ChCl. The mixtures ChCl(ASA) and $ChCl(ASA)_2$ were stable and liquid at room temperature. ChCl(ASA) was diluted with MeOH, in the same proportion as $ChCl(ASA)_2$, to reduce its viscosity. It must be mentioned that ChCl(ASA) was prepared for the first time by another research group as a liquid formulation of an API (active pharmaceutical ingredient) to enhance the bioavailability and rate of delivery of the drug.[33]

Selection of the extraction solvent. The selection of the extraction solvent was decided by planning a series of parallel tests to compare the extraction yields of $ChCl(ASA)_2MeOH$, ChCl(ASA)MeOH and $ChCl(Ph)_3$. To this end, 100 µL of extractant and 500 µL of THF were quickly injected into the aqueous sample (5 mL spiked with pesticides at 2 µg L^{-1}) and the dispersion was vortexed for 2 min. However, after centrifugation, $ChCl(ASA)_2$ and ChCl(ASA) settled at the bottom of the falcon tube, while $ChCl(Ph)_3$ floated on the aqueous sample. Once taken with a micro-syringe, 10 µL were directly injected into the HPLC-MS apparatus (these mixtures cannot be evaporated to dryness). From the comparison of the average value of the areas (3 replicates per type of neoteric solvent), $ChCl(ASA)_2$ showed superior extraction efficiency for the more polar analytes (lower logPs), $ChCl(Ph)_3$ for the least polar ones (higher logPs), while ChCl(ASA) displayed generally lower values. Finally, $ChCl(ASA)_2$ was chosen for both its good performance (see **Figure S-2**) and significantly lower toxicity ($LD_{50\ ASA}$ = 1124 mg Kg^{-1}; $LD_{50\ Ph}$ = 660 mg Kg^{-1}).

Characterization of the $ChCl(ASA)_2$ mixture.

Density measurement. Due to its high viscosity, the mixture was heated up to 80 ° C, taken with a pipette and quickly introduced into a 1-mL flask. Then, it was allowed to cool to room temperature and the sample volume checked for possible contraction. 1 mL of $ChCl(ASA)_2$ was weighed on a microbalance (OHAUS DV215CD Discovery Semi-Micro and Analytical Balance 81 g/210 g capacity, 0.01 mg/0.1 mg readability). Density was calculated as the mean of three replicates:

$\rho = m/V = 1.20 \pm 0.01$ g mL^{-1} (eq. 1)

Density was greater than that of water, in accordance with values found for other DESs/LTTMs[34] and with our experimental observations, i.e. sedimentation of $ChCl(ASA)_2$ after the centrifugation step of the DLLME procedure.

Thermogravimetric analysis. TGA and differential TGA (DTGA) curves and of ChCl, ASA, and $ChCl(ASA)_2$ are displayed in **Figure 3**, while the temperatures in correspondence of a 10 % weight loss ($T_d^{10\%}$) and of the DTGA peaks (T_p^{I} and T_p^{II}) are reported in **Table 2**.

As reported in literature,[35,36] ChCl starts to decompose at about 320 °C, meanwhile ASA showed a two decomposition steps, the first beginning at about 180 °C and the second at 350 °C.

The neoteric solvent had the main weight loss at an intermediate temperature (257 °C). At higher temperature, the second decomposition process occurred approximately at T_p^{II} of ASA and can be attributed to small amount of SA, possibly formed by deacetylation during the $ChCl(ASA)_2$ heating scan or during the LTTM preparation.[37]

Differential scanning calorimetry (DSC). **Figure 4** shows the thermogram of $ChCl(ASA)_2$ obtained in the cooling and heating scans. In both runs only an intense glass transition at -37 ° C (midpoint) was observed (vertical bars in **Figure 4**). The specific heat variation at the glass transition was about 6 J g^{-1} K^{-1}. Under the employed experimental conditions, the sample did not undergo a phase transition, crystallization or melting, and, therefore, it can be defined as a LTTM.

ATR-FTIR spectroscopy. IR spectroscopy is a suitable technique able to study DES and LTTM intra- and inter-molecular H-bonds. The effects of these interactions involve mainly the 4000-2000 cm^{-1} and 1800-1500 cm^{-1} spectral regions, where the O-H and C=O stretching modes occur. In

Figure 5A, the spectra of $ChCl(ASA)_2$ and the parent moieties, ChCl and ASA, are reported. Because of their crystalline nature, ChCl and ASA show particularly complex spectra in the lower wavenumber region, very different from that of the amorphous neoteric solvent.

For sake of clarity, the O-H stretching region (3700-2100 cm^{-1}) is displayed in detail in **Figure 5B**. The IR spectrum of ChCl presents a strong and sharp absorption band centered at 3218 cm^{-1}, assigned to the O-H···Cl^- stretching in the crystalline phase[38] (**Figure 5B**). The stretching region of ASA between 3100 and 2400 cm^{-1} is characterized by a complex structure of overlapped bands, due to strongly hydrogen bonded dimers.[39] $ChCl(ASA)_2$ shows an absorption centered at 3255 cm^{-1}, replacing the strong O-H···Cl^- signal of ChCl at 3218 cm^{-1}. The broadening and blue-shift of the band are due to the H-bond between the ChCl alcoholic and ASA carboxyl as well as ester groups, weaker than that in the ChCl crystal lattice. The $ChCl(ASA)_2$ absorptions between 3100 and 2400 cm^{-1} are similar to those of carboxylic O-H stretching of ASA. Because of their complexity, detailed attribution of the signals cannot be done. The small differences can arise from the different amorphous and crystalline states of the samples. However, it can be presumed that the red-shift observed at the lower wavenumbers could occur because of the formation of strong OH…Cl^- H-bonds between ASA and ChCl.

The 1830-1620 cm^{-1} spectral region, where C=O and C=C stretching vibrations resonate, is reported in **Figure 5C**. As expected, ChCl does not absorb at these wavenumbers. ASA sample shows two strong bands located at 1748 cm^{-1} and 1677 cm^{-1}, assigned to the C=O stretching mode of the acetyl and the carboxylic function, respectively[40] and the aromatic C=C stretching at 1605 cm^{-1}. The formation of the $ChCl(ASA)_2$ LTTM leads to a different absorption profile (green spectrum, **Figure 5C**), characterized by three main overlapped bands, located at 1745, 1706 and 1649 cm^{-1}. The first band could be accounted for the shift of acetyl C=O stretching from ASA (1748 cm^{-1}) to the mixture (1745 cm^{-1}). On the other hand, according to literature data,[41] the signal at 1745 cm^{-1} could be also due to the C=O carboxylic stretching of ASA which forms intermolecular H-bonds. The major band located at 1706 cm^{-1}, originally at 1677 cm^{-1} in crystalline ASA, arises from the large

blue-shift of the C=O carboxylic stretching involved in strong H-bonds in $ChCl(ASA)_2$. Lastly, the small band at 1649 cm^{-1}, which cannot be assigned to any of the two components in the mixture, was attributed to the carbonyl stretching of a small fraction of SA, formed by deacetylation of ASA during the formation of the LTTM at 80 °C, whose presence has been already hypothesized from TGA results.

Large-angle X-ray scattering (LAXS).

The radial distribution functions of the mixture of $ChCl(ASA)_2$ and of the liquid mixture of $ChCl(ASA)_2$ diluted with MeOH (1:1.8 molar ratio) are very similar (see **Figure 6**). The strong contribution at ca. 2.4 Å can be modelled with 6 O—O distances, but they can be also ascribed to C—C from stacked phenyl rings or other intermolecular distances as N-(H)-O. Besides the intramolecular distances within Ch, ASA and MeOH, and the 2.4 Å distance, there is a broad peak at ca. 4.7 Å which certainly contains several different intermolecular distances that have not been included in the model as their contribution to the LAXS function can be neglected above θ=4 $Å^{-1}$. Outside 7.5 Å there seems not to be any preferred distances at all, in strong contradiction to e.g. water and DMSO.[42]

Mass spectrometry. Due to its high viscosity, $ChCl(ASA)_2$ was injected (2 µL) into the mass spectrometer after dilution with MeOH (1:1.8 molar ratio). Q1 full scan spectra were acquired in both ionization modes working in flow injection analysis (FIA); the flow rate of the mobile phase (MeOH) was set at 200 µL min^{-1}. According to what observed by IR spectroscopy, the following ion species were identified on MS spectra: $[Ch+ASA-H]^-$ at *m/z* 283, $[Ch+Cl+ASA-H]^-$ at *m/z* 318, $[Ch+ASA+SA-H]^-$ at *m/z* 421, and $[Ch+2ASA]^+$ at *m/z* 464. **Figure S-3** shows the complexed species ChCl(ASA) at *m/z* 318.0; the characteristic isotopic distribution confirms the presence of the chlorine atom. Under the applied analysis conditions, no evidence about the occurrence of the $ChCl(ASA)_2$ adduct was found.

Optimization of the DLLME extraction. The volume of the extracting solvent, type and volume of dispersing solvent, dispersing device (vortex and ultrasound) and time of dispersion were the

parameters investigated to maximize the extraction of the 24 pesticides. Such experiments were carried out using 5 mL of Milli-Q water samples spiked with analytes at 2 μg L^{-1}.

Optimization of the extraction solvent volume. As far as the extracting volume choice is concerned (50, 100, 200, 300 μL of $ChCl(ASA)_2MeOH$), the chromatographic analysis showed that the peaks' areas decreased as the volume of the extractant increased (**Figure S-4a**), obviously due to the lower achieved enrichment factor ($EF \sim V_{water}/V_{settled}$). However, using 50 μL of the mixture, the settled phase was difficult to recover. Therefore, 100 μL was considered the optimal compromise between EF and recoverable volume of the settled phase.

Selection of the dispersing solvents. The dispersing solvent must: *i*) be miscible with both water and extraction solvent; *ii*) assist the extractant dispersion; *iii*) facilitate the analyte extraction from the aqueous to the organic phase. In case of equal performance, the selection of the dispersing solvent should be based on toxicity and cost.

In this study, THF, DMSO, EtOH, AcCN and MeOH were tested as dispersing solvents because of their miscibility in water and ability to solubilize ASA (THF> DMSO> EtOH> AcCN> MeOH). To make a decision, 15 samples (3 replicates per each dispersing solvent) were spiked with analytes and extracted, using 100 μL of $ChCl(ASA)_2MeOH$ and 500 μL of each dispersing solvent. Results showed that the LTTM dispersion was effectively supported by THF, DMSO and EtOH. Although DMSO and EtOH have lower toxicity, THF was chosen for its greater efficiency in assisting both the extractant dispersion and analyte extraction. Probably, the capability of THF in dissolving ASA may explain its higher efficacy compared to that of the other dispersing solvents.

Another critical parameter is the volume of dispersing solvent. Its impact on extraction yields was evaluated testing 0.1, 0.3, 0.5, 1.0, and 1.5 mL of THF (3 replicates per condition). The use of a low volume (0.1 mL) made it problematic the formation of a stable dispersion. On the other hand, volumes higher than 0.5 mL led to a progressive volume increase of the settled phase (up to 90 μL) and, at the same time, to a decrease of EF. For this reason, the best compromise was achieved using

just 1 mL of THF (70 µL of settled phase). The effect of the dispersing solvent on the average area of the chromatographic peaks is shown in **Figure S-4b**.

Dispersion medium and extraction time. The other parameters to evaluate were the device to support the dispersion and the extraction time. Since DLLME can be assisted by both vortex and ultrasound, two replicates per each condition were compared applying the following extraction times: 1, 2 and 4 min. Comparing the mean value of the chromatographic peak areas, the best extraction was obtained by vortexing for 2 min (**Figure S-4c**).

Analytical method validation. Recovery, precision, linearity, sensitivity, limit of detection (LOD), and limit of quantification (LOQ) were evaluated spiking pre-extraction blank samples with the analytes. All the related results are listed in **Tables 3** and **4**.

Matrix-matched calibration curves, LODs and LOQs. Calibration curves were constructed spiking seven 5-mL aliquots of surface water with increasing concentrations of the analytes (0.03, 1, 10, 20, 30, 40, 50 µg L^{-1}). Extraction and analysis were carried out according to what described in the Experimental Section. Peak areas were plotted versus spike level by applying the least-square method ($y = mx + q$ as regression model). In this way, for each analyte, the method sensitivity (the curve slope) accounted for both the ES response and analyte loss during sample processing. All the determination coefficients (R^2) were above 0.97 (**Table 3**).

LODs and LOQs were assessed as the spike level detectable and quantifiable with a signal-to-noise ratio of 3 and 10, respectively (six replicates). To this end, blank real samples were fortified pre-extraction with the analytes at decreasing concentrations until to meet the described requirements. LODs spanned from 0.002 µg L^{-1} (azoxystrobine) to 2.3 µg L^{-1} (fludioxonil), depending on extraction efficiency and ES-MS sensitivity (see **Table 3** for all data).

Recovery and precision. To calculate recovery and intra-day precision, five aliquots (5 mL) of natural water were spiked pre-extraction with the pesticides at two concentration levels corresponding to LOQ and 10 LOQ; another aliquot was spiked post-extraction with the same nominal concentrations of the analytes. All of these aliquots were analyzed in the same analytical

session, while other two additional analytical sessions were performed to evaluate inter-day precision. In all cases, relative standard deviation (RSD), expression of the method precision, was ≤ 15 % (see **Table 4**).

Analysis of environmental water samples. The method effectiveness was assessed by analyzing the water samples collected at four different points of the River Tiber in May 2018 and analyzed. The results, averaged in triplicate, are summarized in **Table 5**. The most frequently detected substances in the sampled waters were the dodine and dimetomorph fungicides; all of others were undetected or detected under LOQ and within the permitted limits when established. The distribution of pesticides is more or less uniform, since there was not a significant difference between rural and urban areas.

CONCLUSIONS

In this paper, a novel LTTM was prepared and characterized for the first time in our laboratory; subsequently, it was applied as extracting phase to perform a DLLME procedure. Our study evidenced the amorphous nature of $ChCl(ASA)_2$ and gave preliminary results on the possible intermolecular interactions involved in the LTTM formation. From an analytical point of view, the developed DLLME procedure combines the typical advantages of the micro-extraction technique with those inherent in the use of a neoteric solvent. In fact, the $ChCl(ASA)_2$ mixture is composed of ChCl, an organic substance classified as an essential nutrient, and ASA which, in aqueous medium, slowly hydrolyzes to SA, a vegetable hormone widely diffused in nature. Besides the very good extraction yields, another advantage in using $ChCl(ASA)_2$, as well as any other DES/LTTM/IL, is the low vapor pressure, which prevents a possible alteration of the analyte concentration, due to solvent evaporation, when an extract is not immediately analyzed. This event is probable when DLLME is carried out with a chlorinated solvent, whose use furthermore obliges to an evaporation step because of its limited compatibility with a reversed mobile phase. Although evaporation of a chlorinated solvent is a fast step, the LTTM can be simply diluted with MeOH to increase its

polarity and to be directly analyzed. Last but not least, $ChCl(ASA)_2$ could be considered a THEDES (Therapeutic Deep Eutectic Solvent) since it is composed by an active pharmaceutical ingredient (API) and could represent a different way of delivering ASA, i.e. dermal administration.

FUNDING

The authors thank "Sapienza University" for having funded the research starting up project (protocol number AR118164361EF599).

ASSOCIATED CONTENT

Supporting Information. Additional information as noted in the text. This material is available free of charge via the Internet at http://pubs.acs.org.

AUTHOR INFORMATION

Corresponding Author *E-mail: alessandra.gentili@uniroma1.it. Tel: +39-06-49693230; Fax: + 39-06-490631.

CONFLICT OF INTEREST DISCLOSURE

The authors declare no competing financial interest.

REFERENCES

(1) Smith, E. L., Abbott, A. P., Ryder, K. S. *Chem. Rev.* **2014***, 114*, 11060-11082.

(2) Francisco, M., van den Bruinhorst, A., Kroon, M. C. Angew. Chem. Int. Ed. Engl. **2013**, *52*, 3074-3085

(3) Perales, E., García, C. B., Lomba, L., Aldea, L., García, J. I., Giner, B. *Ecotoxicol. Environ. Saf.* **2016**, *132*, 429-434.

(4) Tomé, L. I., Baião, V., da Silva, W., Brett, C. M. *Appl. Mater. Today* **2018***, 10*, 30-50.

(5) Abbott, A. P., Capper, G., Davies, D. L., Rasheed, R. K., Tambyrajah, V. *Chem. Commun.* **2003,** *1*, 70-71.

(6) Laitinen, H. A., Ferguson, W. S., Osteryoung, R. A. *J. Electrochem. Soc.* **1957**, *104*, 516-520.

(7) Duke, F. R., Iverson, M. L. *J. Phys. Chem.* **1958,** *62*, 417-418.

(8) Gambino, M., Gaune, P., Nabavian, M., Gaune-Escard, M., Bros, J. P. *Thermochim Acta* **1987**, *111*, 37-47.

(9) Ashworth, C. R., Matthews, R. P., Welton, T., Hunt, P. A. *Phys. Chem. Chem. Phys.* **2016**, *18*, 18145-18160.

(10) Abbott, A. P., Capper, G., Davies, D. L., Munro, H. L., Rasheed, R. K., Tambyrajah, V. *Chem. Commun.* **2001**, 19, 2010-2011.

(11) Francisco, M., van den Bruinhorst, A., Kroon, M. C. *Green Chem.* **2012**, *14*, 2153-2157.

(12) Gilli, P., Pretto, L., Bertolasi, V., Gilli, G. *Acc. Chem. Res.* **2008**, *42*, 33-44.

(13) Durand, E., Lecomte, J., Villeneuve, P. *Biochimie* **2016**, *120*, 119-123.

(14) Cunha, S. C., Fernandes, J. *Trends Analyt Chem*. **2018**, *105*, 225-239

(15) Khezeli, T., Daneshfar, A., Sahraei, R. *J. Chromatogr. A* **2015***, 1425*, 25-33.

(16) Khezeli, T., Daneshfar, A., Sahraei, R. *Talanta* **2016**, *150*, 577-585.

(17) Farajzadeh, M. A., Mogaddam, M. R. A., Aghanassab, M. *Anal. Methods* **2016**, *8*, 2576-2583.

(18) Farajzadeh, M. A., Sattari Dabbagh, M., & Yadeghari, A. *J. Sep. Sci.* **2017***40*(10), 2253-2260.

(19) Wang, H., Hu, L., Liu, X., Yin, S., Lu, R., Zhang, S., Zhou, W., Gao, H. *J. Chromatogr. A* **2017**, *1516*, 1-8.

(20) Lamei, N., Ezoddin, M., Abdi, K. *Talanta* **2017**, *165*, 176-181.

(21) Yousefi, S. M., Shemirani, F., Ghorbanian, S. A. *Talanta* **2017**, *168*, 73-81.

(22) Aydin, F., Yilmaz, E., Soylak, M. *Microchem. J.* **2017**, *132*, 280-285.

(23) Zeng, H., Qiao, K., Li, X., Yang, M., Zhang, S., Lu, R., Li, J., Gao, H., Zhou, W. *J. Sep. Sci.* **2017**, *40*, 4563-4570.

(24) Ferrone, V., Genovese, S., Carlucci, M., Tiecco, M., Germani, R., Preziuso, F., Epifano, F., Carlucci, G., Taddeo, V. A. *Food Chem.* **2018,** *245*, 578-585.

(25) Rezaee, M., Assadi, Y., Hosseini, M. R. M., Aghaee, E., Ahmadi, F., Berijani, S. *J. Chromatogr. A* **2006**, *1116*, 1-9.

(26) Johansson, G., Sandström, M. *Chem. Scr.* **1973**, *4*, 195-198.

(27) Stålhandske, C. M. V., Persson, I., Sandström, M., Kamienska-Piotrowicz, E. *Inorg. Chem*. **1997**, *36*, 3174-3182.

(28) International Tables for X-ray Crystallography; Kynoch Press: Birmingham, U.K., **1974**, Vol. 4.

(29) Cromer, D. T. *J. Chem. Phys.* **1969**, *50*, 4857-4859

(30) Cromer, D. T.; Mann, J. B. *J. Chem. Phys.* **1967**, *47*, 1892-1894.

(31) Molund, M., Persson, I. *Chem. Scr.* **1985**, *25*, 197-197.

(32) Levy, H. A., Danford, M. D., Narten, A. H. Technical Report ORNL-3960; Oak Ridge National Laboratory: Oak Ridge, TN, **1966**.

(33) Aroso, I. M., Silva, J. C., Mano, F., Ferreira, A. S. D., Dionísio, M., Sá-Nogueira, I., Barreiros, S., Reis, R. L., Paiva, A., Duarte, A. R. C. Eur. J. Pharm. Biopharm. **2016,** *98*, 57–66.

(34) Craveiro, R., Aroso, I., Flammia, V., Carvalho, T., Viciosa, M. T., Dionísio, M., Barreiros, S., Reis, R. L., Duarte, A. R. C., Paiva, A. *J. Mol. Liq.* **2016**, *215*, 534-540.

(35) Chemat, F., Anjum, H., Shariff, A. M., Kumar, P., & Murugesan, T. *J. Mol. Liq.* **2016**, *218*, 301-308.

(36) Ribeiro, Y. A., Caires, A. C. F., Boralle, N., & Ionashiro, M. *Thermochim. Acta* **1996**, *279*, 177-181.

(37) Reepmeyer, J. C. *J. Pharm. Sci.* **1983**, *72*, 322-323.

(38) Perkins, S. L., Painter, P., & Colina, C. M. *J. Phys. Chem. B* **2013**, *117*, 10250-10260.

(39) Boczar, M., Wójcik, M. J., Szczeponek, K., Jamróz, D., Zięba, A., & Kawałek, B. *Chem. Phys.* **2003,** *286*, 63-79.

(40) Binev, I. G., Stamboliyska, B. A., & Binev, Y. I. *J. Mol. Struct.* **1996**, *378*, 189-197.

(41) Champeau, M., Thomassin, J. M., Jérôme, C., & Tassaing, T. *J. Chem. Eng. Data* **2016**, *61*, 968-978.

(42) G. Krakowiak, J. Lundberg, D.; Persson, I. *Inorg. Chem.* **2012**, *51*, 9598-9609.

Caption to figures

Figure 1. Schematic illustration of the DLLME procedure using $ChCl(ASA)_2MeOH$ as extractant.

Figure 2. Photograph of the LTTMs prepared for this study.

Figure 3. TGA (A) and DTGA (B) curves of ASA, ChCl and $ChCl(ASA)_2$ samples recorded at 10 °C min^{-1}.

Figure 4. Cooling and heating DSC profiles of $ChCl(ASA)_2$ recorded at 10 °C min^{-1}. The vertical lines indicate the glass transition temperature T_g at midpoint.

Figure 5. ATR-FTIR spectra of ChCl, ASA and $ChCl(ASA)_2$ in 3700-650 cm^{-1} (A), 3700-2100 cm^{-1} (B) and 1830-1520 cm^{-1} (C) spectral regions.

Figure 6. Top: LAXS radial distribution curves for $ChCl(ASA)_2$ and liquid mixture of $ChCl(ASA)_2$ diluted with MeOH ($ChCl(ASA)_2$ - MeOH 1:1.8 molar). The experimental radial distribution functions $D(r)4\pi r^2 \rho_o$ are shown for $ChCl(ASA)_2$ (blue line) and $ChCl(ASA)_2$ diluted with MeOH (cyan line) together with the sum of model contributions (red line for $ChCl(ASA)_2$ and orange line for $ChCl(ASA)_2$ diluted with MeOH) and the difference (dark gree line for $ChCl(ASA)_2$ and orange line for $ChCl(ASA)_2$ diluted with MeOH). Bottom: Reduced LAXS intensity functions $s \cdot i(s)$ (blue line for $ChCl(ASA)_2$ and cyan line for $ChCl(ASA)_2$ diluted with MeOH) and models$\cdot i_{calc}(s)$ (red line for $ChCl(ASA)_2$ and orange line for $ChCl(ASA)_2$ diluted with MeOH).

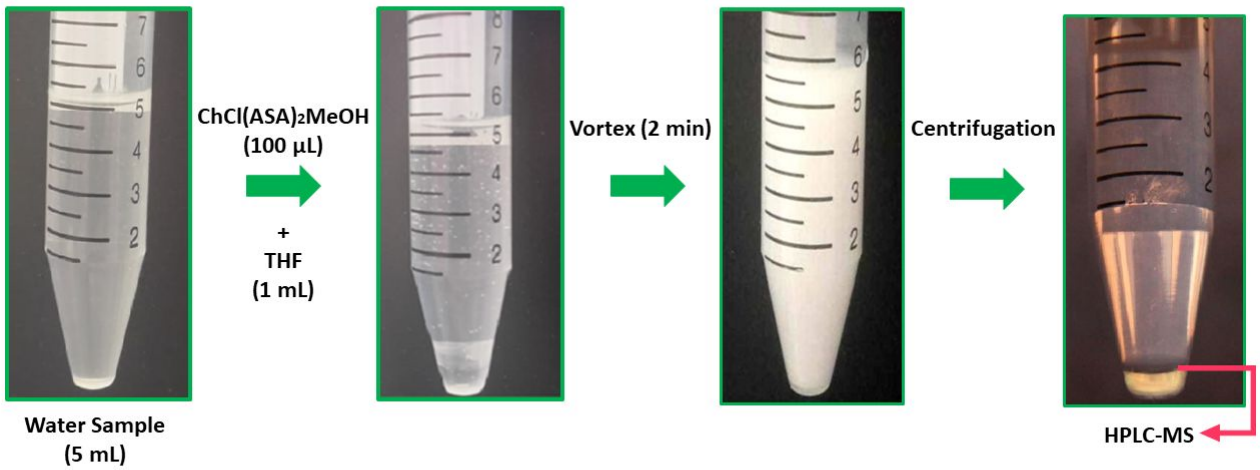
Water Sample
(5 mL)
ChCl(ASA)2MeOH
(100 µL)
+
THF
(1 mL)
Vortex (2 min)
Centrifugation
HPLC-MS

Figure 1

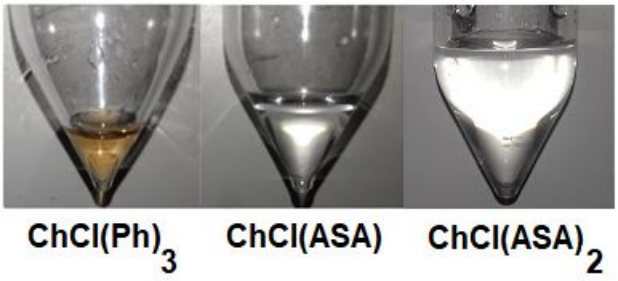

Figure 2

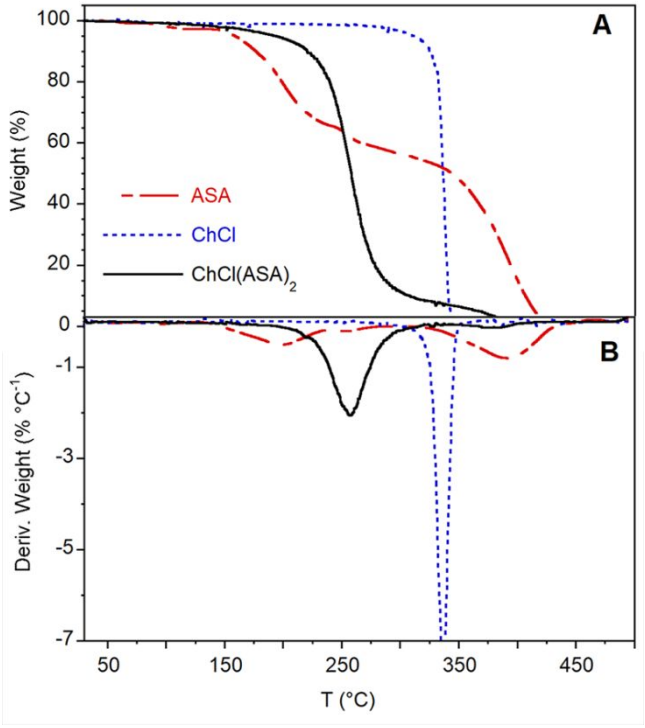
A
B
Weight (%)
Deriv. Weight (% °C-1)
T (°C)
ASA
ChCl
ChCl(ASA)2
100
80
60
40
20
0
-1
-3
-5
-7
50
150
250
350
450

Figure 3

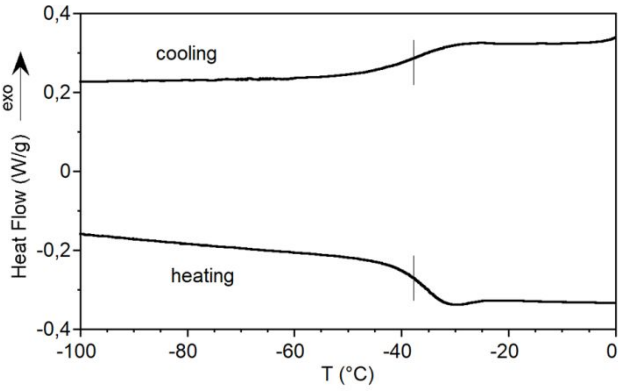
0,4
0,2
0
-0,2
-0,4
cooling
heating
exo
Heat Flow (W/g)
-100
-80
-60
-40
-20
0
T (°C)

Figure 4

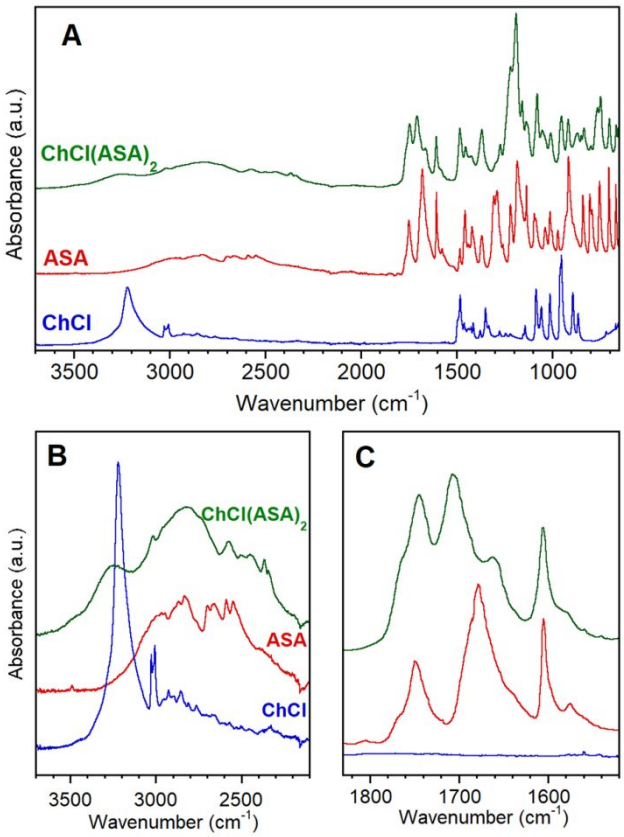
A
ChCl(ASA)2
ASA
ChCl
Absorbance (a.u.)
3500
3000
2500
2000
1500
1000
Wavenumber (cm-1)
B
C
ChCl(ASA)2
ASA
ChCl
Absorbance (a.u.)
3500
3000
2500
Wavenumber (cm-1)
1800
1700
1600
Wavenumber (cm-1)

Figure 5

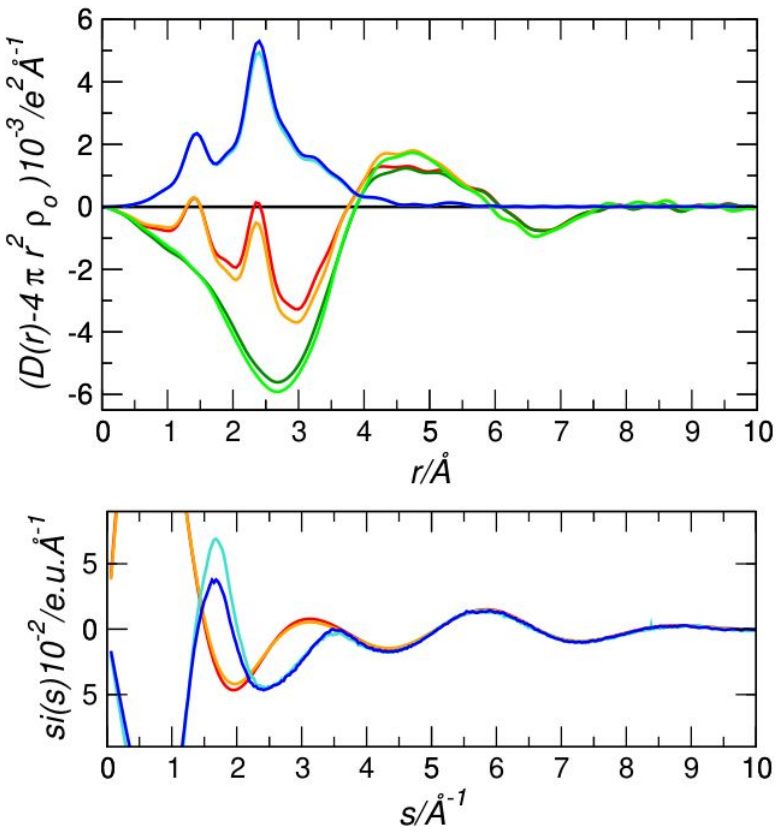

Figure 6

Table 1. Conditions for preparation of some DESs/LTTMs

Components		Molar ratio	Temperature of preparation (°C)
Hydrogen-Bond Acceptor (HBA)[a]	**Hydrogen-Bond Donor (HBD)**[b]		
Choline chloride	phenol	1:3	ambient
Choline chloride	salycilic acid	1:1	80°C
Choline chloride	salycilic acid	1:2	80°C
Choline chloride	acetylsalycilic acid[c]	1:1	80°C
Choline chloride	acetylsalycilic acid[c]	1:2	80°C

[a] $T_{melting\ HBA}$: 302°C. [b] $T_{melting\ HBD}$: 41 °C (phenol), 135°C (acetylsalycilic acid), 159°C (salycilic acid).

Table 2. Thermogravimetric analysis results of ASA, ChCl and ChCl(ASA)$_2$ samples.

Sample	T_d^{10} (°C)	T_p^{1} (°C)0	T_p^{II} (°C)
ASA	177	200	390
ChCl	320	336	-
ChCl(ASA)$_2$	225	257	378

Table 3. Regression parameters, LODs and LOQs for the selected pesticides.

Standard	Matrix-matched calibration curve (y=ax+b)	R^2	LODs	LOQs
			µg L^{-1}	
Imidacloprid	y = 21 x + 21	0.9905	0.04	0.1
Acetamiprid	y = 87 x +62	0.9961	0.01	0.04
Dodine	y = 68 x + 58	0.9890	0.02	0.08
Methyl-thiophanate	y = 133 x -1	0.9975	0.005	0.02
Dimetomorph	y = 67 x - 91	0.9737	0.003	0.009
Spirotetramat	y = 263 x +203	0.9900	0.009	0.03
Fludioxonil	y = 0.7 x + 0.6	0.9911	2.3	7.7
Azoxystrobine	y = 337 x + 494	0.9863	0.002	0.006
Myclobutanil	y = 90 x + 84	0.9910	0.003	0.01
Boscalid	y =40 x + 68	0.9861	0.01	0.05
Tebuconazole	y = 166 x + 240	0.9897	0.003	0.009
Fluquinconazole	y = 77 x + 123	0.9896	0.01	0.05
Methoxyfenozide	y = 258 x + 228	0.9967	0.01	0.04
Penconazole	y = 76 x + 106	0.9924	0.008	0.03
Propiconazole	y = 97 x + 117	0.9947	0.02	0.07
Pyraclostrobin	y = 37 x + 9	0.9808	0.01	0.04
Clofentezine	y = 16 x + 15	0.9759	0.08	0.3
Buprofezin	y = 277 x + 105	0.9973	0.004	0.01
Chlorpyrifos-methyl	y = 3 x + 1	0.9849	0.3	0.9
Tebufenpyrad	y = 35 x + 29	0.9833	0.02	0.06
Pyriproxyfen	y = 301 x + 455	0.9812	0.003	0.01
Chlorpyrifos	y = 3 x + 4	0.9772	0.2	0.7
Hexythiazox	y = 19 x – 6	0.9853	0.03	0.1
Pyridaben	y = 17 x – 1	0.9975	0.04	0.1

Table 4. Recovery and precision for the selected pesticides.

Standard	Recovery (intra-day precision)		Interday precision	
	Spike level		Spike level	
	LOQ	10 LOQ	LOQ	10 LOQ
Imidacloprid	22 (6)	21 (12)	12	14
Acetamiprid	29 (13)	18 (10)	9	12
Dodine	80 (7)	81 (7)	9	9
Methyl-thiophanate	61 (8)	70 (15)	13	15
Dimetomorph	83 (10)	85 (7)	10	9
Spirotetramat	80 (14)	79 (8)	14	10
Fludioxonil	91 (12)	83 (9)	12	12
Azoxystrobine	88 (10)	80 (6)	14	13
Myclobutanil	71 (13)	76 (3)	14	5
Boscalid	88 (6)	91 (10)	6	12
Tebuconazole	90 (14)	89 (7)	11	9
Fluquinconazole	46 (12)	44 (7)	12	10
Methoxyfenozide	83 (12)	77 (7)	12	8
Penconazole	79 (13)	81 (8)	14	9
Propiconazole	77 (7)	89 (6)	10	8
Pyraclostrobin	68 (13)	56 (7)	13	7
Clofentezine	66 (9)	96 (5)	10	7
Buprofezin	81 (9)	94 (10)	10	11
Chlorpyrifos-methyl	92 (11)	85 (13)	14	13
Tebufenpyrad	49 (3)	88 (4)	5	6
Pyriproxyfen	87 (11)	74 (9)	12	10
Chlorpyrifos	91 (12)	73 (10)	12	12
Hexythiazox	92 (9)	81 (13)	10	14
Pyridaben	90 (11)	71 (8)	12	10

Table 5. Levels of some pesticides (μg L^{-1}) found in the four sampling sites along the River Tiber basin (Central Italy)[a]

Analytes	Oasis of Farfa	Tor di Quinto	Tiber Island	Marconi
	(μg L^{-1})			
Dodine	< LOQ	2.04 ± 0.06	0.36 ± 0.01	< LOQ
Methyl-thiophanate	LOQ	n.d.[b]	<LOQ	n.d
Dimetomorph	1.427 ± 0.003	1.927 ± 0.003	1.625 ± 0.006	1.848 ± 0.009
Azoxystrobine	< LOQ	< LOQ	< LOQ	<LOQ
Tebuconazole	< LOQ	< LOQ	<LOQ	<LOQ

[a] Results are given as the average of three replicate assays ± SD; [b] n.d.: not detected

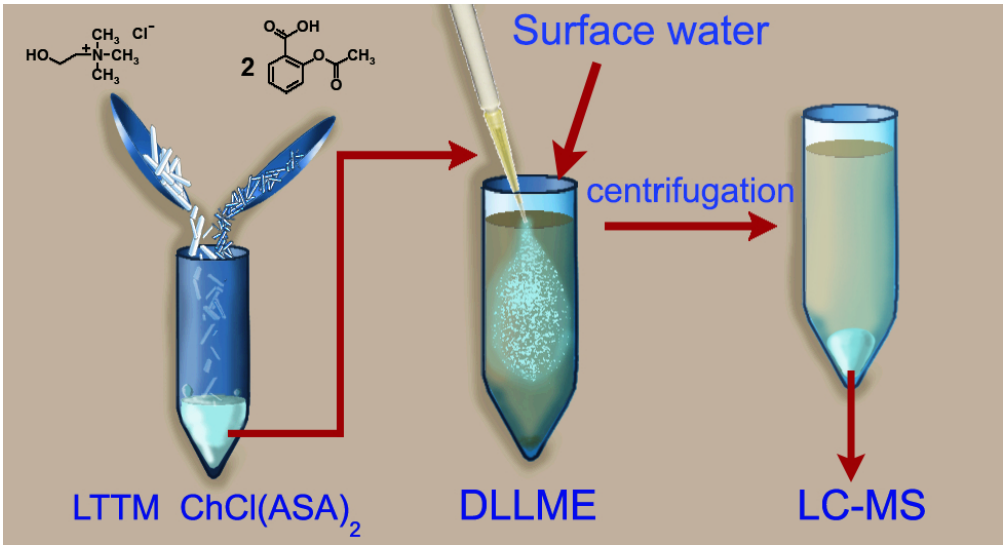

82x44mm (300 x 300 DPI)